

Effect of Synthesis and Sintering Conditions on the Thermoelectric Properties of *n*-Doped Mg₂Si

S. FIAMENI,¹ A. FAMENGO,^{1,4} F. AGRETI,¹ S. BOLDRINI,¹
S. BATTISTON,¹ M. SALEEMI,² M. JOHNSON,³ M.S. TOPRAK,²
and M. FABRIZIO¹

1.—National Research Council of Italy, Institute for Energetics and Interphases, Corso Stati Uniti 4, 35127 Padua, Italy. 2.—Department of Materials and Nano Physics, KTH Royal Institute of Technology, Kista, Stockholm, Sweden. 3.—Department of Materials and Environmental Chemistry, Stockholm University, Stockholm, Sweden. 4.—e-mail: a.famengo@ieni.cnr.it

Magnesium silicide (Mg₂Si)-based alloys are promising candidates for thermoelectric (TE) energy conversion in the middle–high temperature range. The detrimental effect of the presence of MgO on the TE properties of Mg₂Si based materials is widely known. For this reason, the conditions used for synthesis and sintering were optimized to limit oxygen contamination. The effect of Bi doping on the TE performance of dense Mg₂Si materials was also investigated. Synthesis was performed by ball milling in an inert atmosphere starting from commercial Mg₂Si powder and Bi powder. The samples were consolidated, by spark plasma sintering, to a density >95%. The morphology, and the composition and crystal structure of samples were characterized by field-emission scanning electronic microscopy and x-ray diffraction, respectively. Moreover, determination of Seebeck coefficients and measurement of electrical and thermal conductivity were performed for all the samples. Mg₂Si with 0.1 mol% Bi doping had a *ZT* value of 0.81, indicative of the potential of this method for fabrication of *n*-type bulk material with good TE performance.

Key words: Magnesium silicide, thermoelectricity, SPS

INTRODUCTION

Thermoelectric (TE) devices are promising candidates for recycling of waste heat and for power generation. In particular, Mg₂Si-based alloys are interesting materials for TE energy conversion in the middle–high temperature range. TE devices have many advantages, including being silent and portable solid-state devices with no moving parts. Silicide-based TE materials are also very attractive, because they could replace lead-based compounds as a result of their low cost, non-toxicity,^{1,2} and the abundance of their raw materials. Their low density also enables TE generator weight reduction (a key feature for automotive applications).^{3,4}

p-Type Mg₂Si can be produced by doping with Ag and Cu whereas *n*-type can be obtained by doping

with Sb, Al, and Bi.^{5–9} In particular, remarkable TE figures of merit, *ZT*, for *n*-doped Mg₂Si materials have been obtained by using Bi as dopant (*ZT* = 0.86 at approx. 600°C¹⁰). For this reason, in the work discussed in this paper the effect of the amount Bi doping, as *n*-type dopant, on the TE performance of dense Mg₂Si materials was investigated.

Solid-state synthesis of Bi-doped Mg₂Si has previously been achieved by ball milling, thermal treatment, and such sintering procedures as spark plasma sintering (SPS)^{8,10} or hot pressing.¹¹ Thermal treatment seems essential to dope the silicide when starting from Mg₂Si as precursor. In fact, x-ray diffraction (XRD) analysis of ball-milled powder clearly showed the presence of free Bi.¹² Thermal treatment at 600°C under an inert atmosphere promoted doping of the powders, but oxygen contamination also occurred, giving rise to the formation of MgO. Previous research has revealed the

detrimental effect of MgO on the TE properties of Mg₂Si-based materials.^{9,12} For this reason, the purpose of this work was to reduce the MgO content of Mg₂Si-based pellets by optimization of the conditions used for synthesis and sintering. Another purpose of the work was to reduce the total processing time required to obtain TE pellets, by avoiding the powder thermal treatment step after ball milling and before sintering. Hence, synthesis was performed by a planetary milling under an inert atmosphere, starting from commercial Mg₂Si powders and Bi powders; the product was subsequently consolidated by SPS. The sintering conditions were selected on the basis of previous work in which temperature, pressure, and holding time were investigated to achieve high compaction density (>96%).¹³

EXPERIMENTAL

Silicide-based pellets were produced from commercial magnesium silicide powder (325 mesh, 99.5%; Pi-Kem, Tamworth, UK) and Bi powder (325 mesh, 99.5%; Alfa Aesar, Karlsruhe, Germany).

Raw Mg₂Si powder containing different amounts of Bi was ground under an Ar atmosphere, in a planetary ball mill, with hexane as dispersion medium (WC jar, 330 rpm for 8 h) to obtain samples of composition $x = 0.01, 0.015, 0.02$, and 0.03 , where x is the Bi:Mg₂Si molar ratio. After ball milling, the hexane was evaporated in glove box under an Ar atmosphere and the powders obtained were sintered by SPS (Dr Sinter 2050; Sumitomo Coal Mining, Tokyo, Japan) at 750°C under 75 MPa for 2 min in a graphite die (heating rate 100°C min⁻¹ and free cooling process). All the samples had relative densities >95% compared with the theoretical densities, as evaluated by Rietveld refinement. XRD analyses were performed with a Philips PW 3710 x-ray diffractometer (Koninklijke Philips, Eindhoven, The Netherlands) with Bragg-Brentano geometry and a Cu K α source (40 kV, 30 mA). Rietveld refinement of the XRD profiles was used to obtain information about amounts of phases, crystallite sizes, and lattice parameters.¹⁴

Morphological and compositional characterization was performed by use of a Sigma Zeiss (Carl Zeiss, Oberkochen, Germany) field emission-scanning electron microscope (FE-SEM).

The thermal diffusivity and specific heat of the samples were measured by use of a laser flash thermal diffusivity apparatus (LFA 457 MicroFlash; Netzsch, Selb, Germany). The specific heat was obtained by comparison with a standard material (Pyroceram 9606 by Netzsch). The thermal conductivity κ was calculated by use of the formula $\kappa = a\rho C_p$ where a is the thermal diffusivity, ρ the density and C_p the specific heat of the material.

The carrier concentrations were determined at room temperature (RT), by means of Hall effect measurements on dense Mg₂Si pellets, by use of a

Keithley (Cleveland, OH, USA) 2636 sourcemeter and Keithley 2182 nanovoltmeter. Measurement was performed in a magnetic field of approximately 370 mT. Mobility was evaluated by measuring electrical resistivity by the Van der Pauw method, by converting the setup mentioned above for Hall measurement to Van der Pauw geometry.

The Seebeck coefficient and the electrical conductivity were measured in the temperature range from RT to 600°C by use of a custom test apparatus described elsewhere.¹⁵ All measurements were performed under an Ar atmosphere.

RESULTS AND DISCUSSION

XRD analysis of the ball-milled powders revealed the presence of free Bi and no Mg₂Si peak shift, as observed in previous work.¹² The MgO content was below 1 wt.% for both the pristine material and the ball-milled powders.

Figure 1 shows the XRD patterns obtained from undoped Mg₂Si and from Bi-doped Mg₂Si pellets ($x = 0.01, 0.015, 0.02$) after SPS. Rietveld refinement of the XRD data¹⁴ revealed that all the samples contained Mg₂Si as the major crystalline phase; small amounts of MgO and Si were also detected (Table I). The amount of MgO was approximately 3 wt.% in undoped Mg₂Si and between 3 and 7 wt.% in Bi-doped samples. Moreover, the presence of two Mg₂Si phases with different cell parameters, because of different dopant content, was clearly apparent for all the doped sintered samples. As an example, Fig. 2 shows two Mg₂Si reflections, at 440° and 531°, for the sample with $x = 0.02$, for which the contributions to the peak shapes for the two phases is particularly evident. Table I lists the results obtained from Rietveld refinement of the XRD profiles for the two Mg₂Si phases. For the first phase the cell parameter was 6.357 ± 0.001 Å whereas for the other phase the cell parameter was larger (6.367 ± 0.003 Å), which

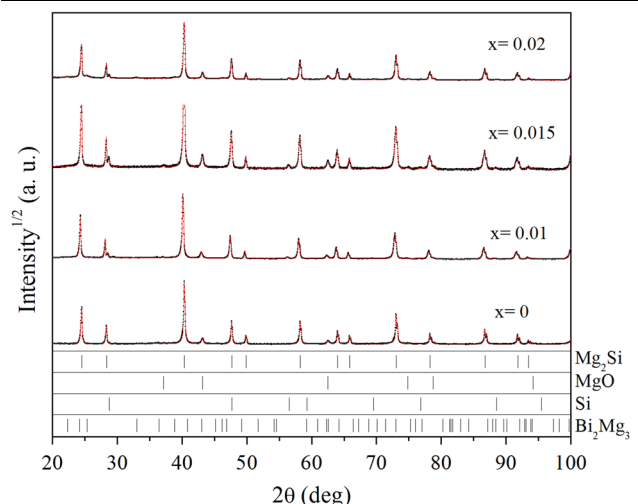
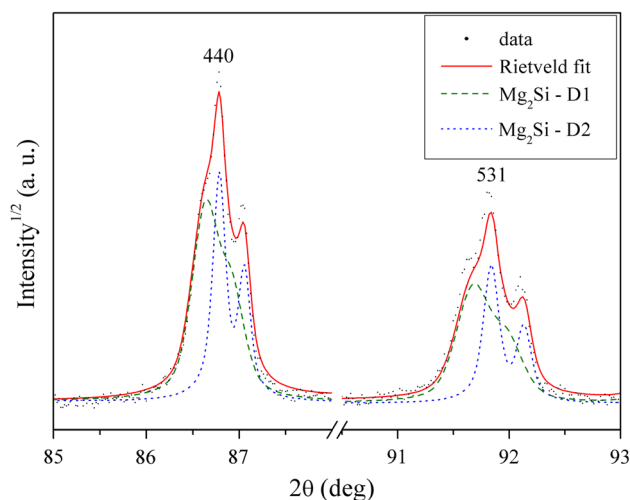
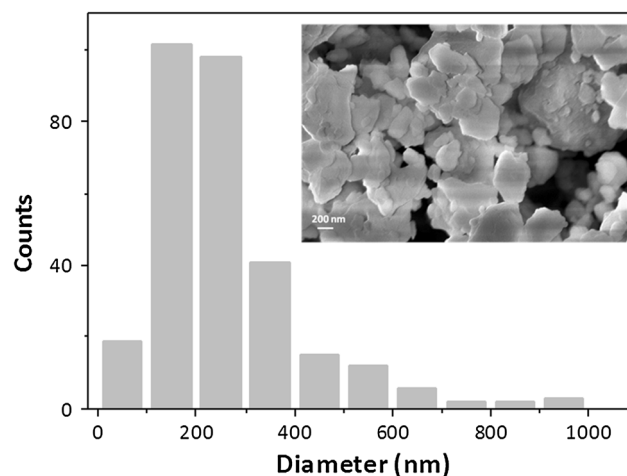


Fig. 1. XRD patterns of sintered samples containing different amounts of Bi.

Table I. Phase content of all the samples, as obtained by Rietveld refinement of XRD data. Samples contained two Mg₂Si phases (D1 and D2) with different Bi doping levels

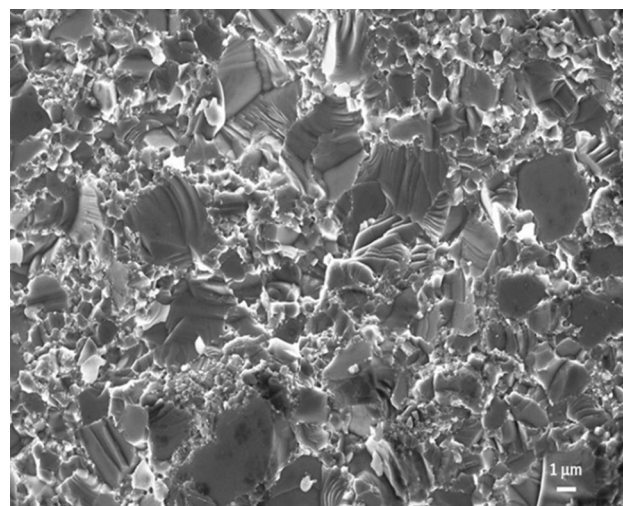
Sample	Phase	wt.%	Mg ₂ Si (wt.%)	MgO (wt.%)	Si (wt.%)	Bi ₂ Mg ₃ (wt.%)
$x = 0$	Mg ₂ Si D1	96.7	96.7 ± 0.5	3.3 ± 0.2		
	Mg ₂ Si D2					
$x = 0.01$	Mg ₂ Si D1	64.7	94.6 ± 1.5	4.1 ± 0.3	1.3 ± 0.2	
	Mg ₂ Si D2					
$x = 0.015$	Mg ₂ Si D1	45.9	90.3 ± 0.7	7.1 ± 0.2	2.6 ± 0.1	
	Mg ₂ Si D2					
$x = 0.02$	Mg ₂ Si D1	36.6	92.7 ± 1.5	5.1 ± 0.3	1.4 ± 0.1	<1
	Mg ₂ Si D2					

Fig. 2. Contributions to the peak shapes of the two different Mg₂Si phases (D1 and D2) for the sample with $x = 0.02$.Fig. 3. FE-SEM image of undoped Mg₂Si powder and particle size analysis.

corresponds to greater Bi doping of the magnesium silicide. The ratio of the weight of the former doped phase (D1 in Table I) to that of the latter doped phase (D2 in Table I) increased with increasing the amount of Bi. These results show how the reported synthesis gave rise to composite materials in which Mg₂Si was inhomogeneously doped. Indeed, the fast sintering process could have prevented complete diffusion of Bi through the magnesium silicide grains.

The sample with $x = 0.03$ had poor mechanical properties after SPS. Three samples with $x = 0.03$ were sintered, but all samples obtained were broken. This behavior, and similar behavior previously observed for Bi-doped samples with $x = 0.04$,¹² showed that Bi content > 2 at.% resulted in high brittleness of Mg₂Si-based TE samples, probably because of the presence of free Bi at grain boundary.

FE-SEM was used to study the grain size of the ball-milled powders and sintered pellets. The particle sizes of ball-milled powders were mainly between 200 and 300 nm for all samples. As an example, the FE-SEM image of undoped Mg₂Si powder, with results from particle-size analysis (Image J software), is shown in Fig. 3. Figure 4

Fig. 4. FE-SEM image of Bi-doped Mg₂Si ($x = 0.02$) after SPS.

shows the grain size and high density typical of all sintered samples.

Electrical properties of these samples, i.e. charge carrier concentrations and electrical mobility of the

Table II. Charge carrier concentrations and mobility at RT at different Bi contents

Sample	Carrier concentration ($\times 10^{19} \text{ cm}^{-3}$)	Mobility ($\text{cm}^2 \text{ V}^{-1} \text{ s}^{-1}$)
$x = 0$	0.50	205
$x = 0.010$	3.16	31.3
$x = 0.015$	3.56	28.7
$x = 0.020$	4.14	32.7

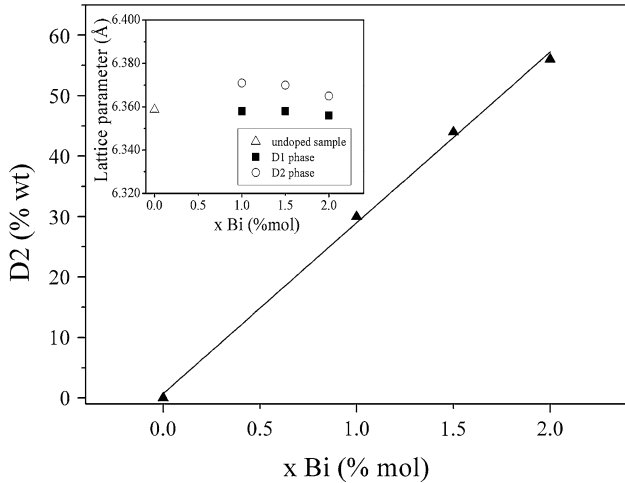


Fig. 5. Correlation between nominal Bi content molar percentage and weight percentage of the Mg_2Si phase with higher Bi-doped level (D2; Table I) calculated by Rietveld refinement of the XRD data. The black line is the result from linear fitting of the experimental points. Inset: lattice parameters for the two phases with different Bi doping levels, D1 (solid square) and D2 (void circles), as a function of the nominal Bi content.

undoped and Bi-doped Mg_2Si , are reported in Table II. The carrier concentrations were lower than those reported in the literature for Bi-doped Mg_2Si .¹⁶ The highest mobility was that of undoped Mg_2Si . The doped samples seemed not to be affected by the nominal concentration of Bi and their mobilities were lower than those reported in the literature.¹⁶ The trend and values of the carrier concentrations and mobilities were probably affected by the presence of the two distinct doped phases and the derived lattice disorder.

The correlation between nominal Bi content and the quantity of the Mg_2Si phase with the higher Bi content (D2) (Table I) is reported in Fig. 5. The trend is clearly linear, indicating the amount of the D2 phase was increased by adding increasing quantities of Bi to the Mg_2Si powder. The inset in Fig. 5 shows the variation of the lattice parameter a versus nominal Bi content for both Mg_2Si phases. The lattice parameter for the D2 phase did not increase with nominal Bi content, as expected when the material is doped with increasing amounts of Bi.¹¹ This could indicate that the dopant concentrations in the doped phases were nearly the same (probably near the solution limit) for the three

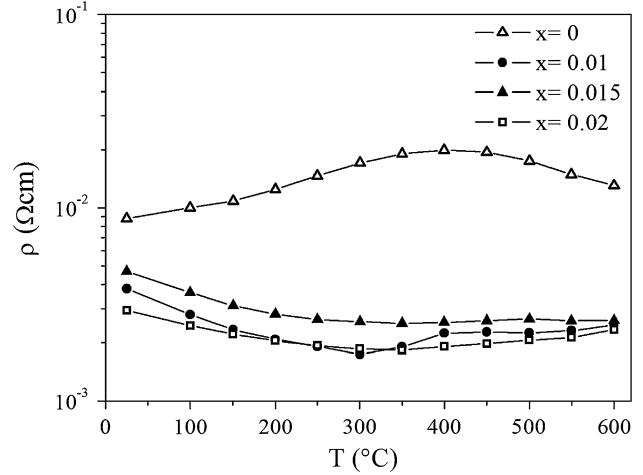


Fig. 6. Electrical resistivity, ρ , of Bi-doped and undoped Mg_2Si as a function of temperature.

samples, in agreement with the similar mobility found for the three dopant concentrations. Thus, increasing the amount of Bi increased the mass percentage of the D2 phase. With regard to the D1 phase, the lattice parameter was approximately the same, as a function of Bi content, very close to that for undoped Mg_2Si . This means that D1 had a lower Bi content and could be regarded as undoped.

Figure 6 shows the temperature dependence of the electrical resistivity (ρ) of undoped Mg_2Si and Bi-doped samples. ρ for all the Bi-doped samples gradually decreased with increasing temperature up to 300°C, indicating semiconductor-like behavior,^{11,12,17} and increased slightly from 350°C to 600°C. As reported by Bux et al.,¹⁶ the carrier concentration of Bi-doped Mg_2Si is nearly constant across the entire temperature range considered. The increase of ρ in the range 350–600°C could be attributable to the decrease of the carrier mobility, limited by phonon scattering phenomena, as previously reported.^{10,16,18} All the doped samples had comparable ρ values at 600°C. In contrast, ρ values of undoped Mg_2Si increased up to 400°C and then decreased. The decrease of ρ at high temperatures is consistent with the intrinsic conduction associated with the band gap of 0.77 eV for Mg_2Si .^{10,19} The ρ values of all the samples were lower than those previously obtained for Bi-doped samples,¹² mainly because of the lower MgO content (3–7 wt.% instead of 30 wt.%). The lower ρ values for the samples with

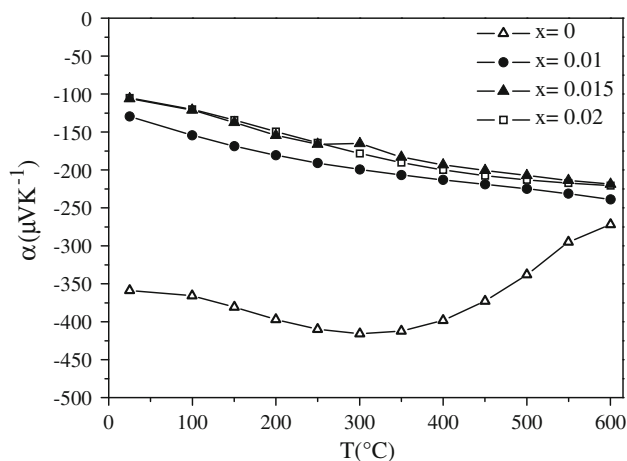


Fig. 7. Seebeck coefficients of undoped and Bi-doped Mg₂Si as a function of temperature.

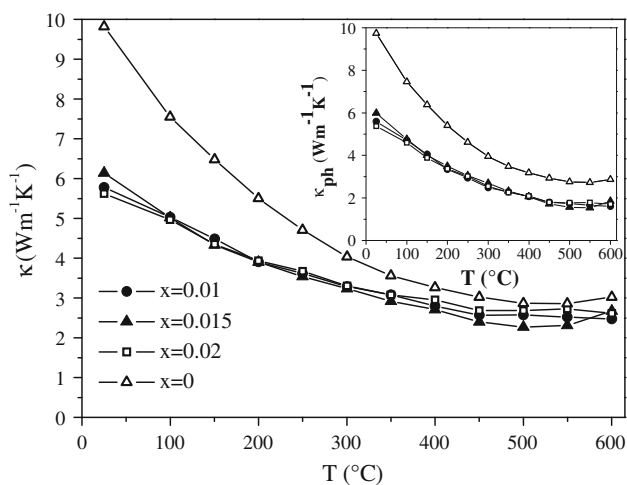


Fig. 8. Total thermal conductivities. Inset: lattice thermal conductivity of undoped and Bi-doped Mg₂Si as a function of temperature.

lower MgO content further confirms the detrimental effect of MgO on the electrical conductivity of Bi-doped magnesium silicides, as reported elsewhere.¹² The higher resistivity of the sample with $x = 0.015$ could be related to its higher MgO content.

Figure 7 reports the Seebeck coefficients (α) of undoped and doped samples as a function of temperature. The sign of Seebeck coefficient was negative, indicative of typical *n*-type behavior of Bi-doped Mg₂Si. The temperature dependence was nearly linear, typical of an extrinsic-doped semiconductor.¹⁶ The α values were consistent with those previously reported for this kind of material.^{11,12}

The thermal conductivities (κ) of all sintered samples, reported in Fig. 8, decreased with increasing temperature, in accordance with literature data.^{8,10,11} The lattice (κ_{ph}) and electronic (κ_{el}) contributions can be separated by the Wiedemann–Franz law ($\kappa_{\text{el}} = L\sigma T$), where σ is the electrical

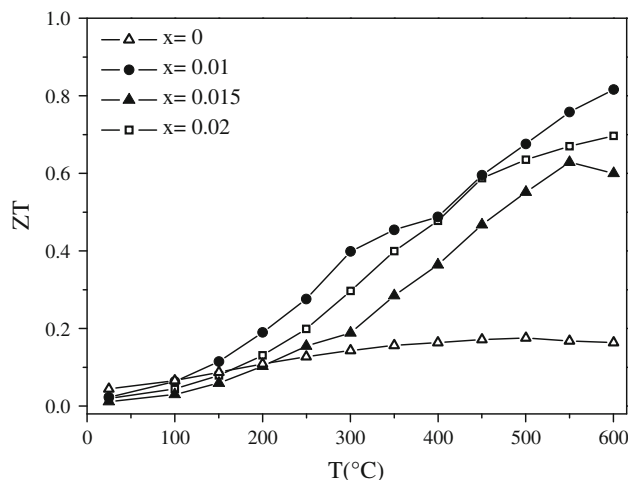


Fig. 9. Figure of merit (ZT) of undoped and Bi-doped Mg₂Si as a function of temperature.

conductivity and the Lorenz number, L , is assumed to be constant ($L = 2.45 \times 10^{-8} \text{ V}^2 \text{ K}^{-2}$). The inset in Fig. 8 shows the change of lattice thermal conductivity as a function of temperature. As expected, the κ_{ph} contribution was largely predominant. All the doped samples had similar values at 600°C and the nominal Bi-amount did not seem to affect κ values over the whole temperature range. However, the thermal conductivities of the doped samples were lower than for undoped Mg₂Si. On the basis of these results, it is possible to assert that the doping used in this work effectively reduced the thermal conductivity. Furthermore, the κ values measured in this work were very similar to those reported elsewhere^{10,16} for heavy and uniform Mg₂Si doping.

Figure 9 shows the temperature dependence of the figure of merit of the undoped and Bi doped samples. ZT increased with increasing temperature, as previously reported for these materials.^{8,10–12} The maximum ZT value of 0.81 at 600°C was obtained for the sample with $x = 0.01$. This value was consistent with those previously reported for this kind of material,^{10,16} suggesting that the presence of the two Mg₂Si phases (D1 and D2) did not dramatically affect the TE properties of Bi-doped Mg₂Si.

Considering the structural features and properties discussed above, it is reasonable to suggest two possible models for the presence of the two phases in the materials obtained in this work. All the samples underwent direct fast SPS, without prior thermal treatment. Presumably, Bi atoms had insufficient time to diffuse throughout the Mg₂Si grains, forming an exterior Bi-doped layer and leaving the core undoped (D1 phase). Another model could consider that some grains are fully doped and other grains are undoped. On adding more Bi, the number of doped grains increases, explaining the increased amount of D2 (higher-doping-level phase). Both models are consistent with the presence of two Mg₂Si phases and could explain the trends found for

the lattice parameters and D1-to-D2 weight ratio as a function of nominal Bi content. Unfortunately, modeling the electrical and thermal transport properties on the basis of these models is not straightforward and requires further work.

CONCLUSION

We report the synthesis of Bi-doped Mg_2Si starting from commercial Mg_2Si powder and Bi powder. The synthesis and sintering steps were performed with the objective of limiting oxygen contamination. The resulting pellets were characterized by low MgO content and improved TE properties compared with those of Bi-doped Mg_2Si containing larger amounts of MgO. The XRD data showed the presence of two Mg_2Si phases, corresponding to doped and undoped material. For this reason, we conclude that the reported synthetic procedure gave rise to composite materials in which the Mg_2Si is only partially doped, probably because of the rapid sintering process. However, the sample with the molar ratio $x = 0.01$ had a ZT value of 0.81, indicating that, even for non-uniform doping, TE performance is in agreement with that reported in the literature.^{10,16}

Modeling the transport and TE properties of the composite materials described here is not straightforward and further effort is required to better correlate structural features with electrical and thermal properties.

The SPS conditions can be improved to enable complete n -type doping while maintaining low oxygen contamination.

ACKNOWLEDGEMENTS

The authors are grateful to Dr Rosalba Gerbasi for XRD analysis and to Dr Alberto Ferrario for useful technical support and fruitful discussion. This work was funded by the Italian National Research Council—Italian Ministry of Economic

Development Agreement “Ricerca di sistema elettrico nazionale” and in part by the Swedish Foundation for Strategic Research—SSF and Swedish Energy Agency (project no. 36656-1).

REFERENCES

1. D.M. Rowe, *CRC Handbook of Thermoelectrics* (Boca Raton: CRC, 1995).
2. G.J. Snyder and E.S. Toberer, *Nat. Mater.* 7, 105 (2008).
3. T. Nemoto, M. Akasaka, T. Iida, J. Sato, K. Nishio, T. Takei, and Y. Takanashi, *ICT'06, 25th International Conference on Thermoelectrics* (2006), p. 552.
4. J.-I. Tani and H. Kido, *Intermetallics* 32, 72 (2013).
5. M. Akasaka, T. Iida, A. Matsumoto, K. Yamanaka, Y. Takanashi, T. Imai, and N. Hamada, *J. Appl. Phys.* 104, 013703 (2008).
6. T. Sakamoto, T. Iida, A. Matsumoto, Y. Honda, T. Nemoto, J. Sato, T. Nakajima, H. Taguchi, and Y. Takanashi, *J. Electron. Mater.* 39, 1708 (2010).
7. J. Tani and H. Kido, *Intermetallics* 15, 1202 (2007).
8. S.-M. Choi, K.-H. Kim, I.-H. Kim, S.-U. Kim, and W.-S. Seo, *Curr. Appl. Phys.* 11, S388 (2011).
9. S. Battiston, S. Fiameni, M. Saleemi, S. Boldrini, A. Famengo, F. Agresti, M. Stingaciu, M.S. Toprak, M. Fabrizio, and S. Barison, *J. Electron. Mater.* 42, 1956 (2013).
10. J.-I. Tani and H. Kido, *Phys. B. Condens. Matter* 364, 218 (2005).
11. S.-W. You and I.-H. Kim, *Curr. Appl. Phys.* 11, S392 (2011).
12. S. Fiameni, S. Battiston, S. Boldrini, A. Famengo, F. Agresti, S. Barison, and M. Fabrizio, *J. Solid State Chem.* 193, 142 (2012).
13. M. Saleemi, M.S. Toprak, S. Fiameni, S. Boldrini, S. Battiston, A. Famengo, M. Stingaciu, M. Johnsson, and M. Muhammed, *J. Mater. Sci.* 48, 1940 (2013).
14. L. Lutterotti, S. Matthies, H.R. Wenk, A.S. Schultz, and J.W. Richardson Jr, *J. Appl. Phys.* 81, 594 (1997).
15. S. Boldrini, A. Famengo, F. Montagner, S. Battiston, S. Fiameni, M. Fabrizio, and S. Barison, *J. Electron. Mater.* 42, 1319 (2013).
16. S.K. Bux, E.S. Toberer, G.J. Snyder, R.B. Kaner, and J.-P. Fleurial, *J. Mater. Chem.* 21, 12259 (2011).
17. K. Mars, H. Ihou-Mouko, G. Pont, J. Tobola, and H. Scherrer, *J. Electron. Mater.* 38, 1360 (2009).
18. Y. Noda, H. Kon, Y. Furukawa, I.A. Nishida, and K. Masumoto, *Mater. Trans.* 33, 851 (1992).
19. T. Sakamoto, T. Iida, N. Fukushima, Y. Honda, M. Tada, Y. Taguchi, Y. Mito, H. Taguchi, and Y. Takanashi, *Thin Solid Films* 519, 8528 (2011).